






4DATLANTIC-OHC

ALGORITHM THEORETICAL BASIS DOCUMENT

	Name	Organisation	Date	Visa
Written by:	Victor Rousseau Michaël Ablain Robin Fraudeau Florence Marti	Magellium	17/08/2022	
Checked by:	Michaël Ablain	Magellium	17/08/2022	
Approved by:	Gilles Larnicol	Magellium	17/08/2022	
Accepted by:	Jérôme Benveniste	ESA	01/06/2022	

Document reference:	OHCATL-DT-020-MAG_ATBD
Edition.Revision:	1.2
Date Issued:	17/08/2022
Customer :	ESA
Ref. Market, consultation :	AO/1-10546/20/I-NB
Contrat No. :	4000134928/21/I-NB

Distribution List

	Name	Organisation	Nb. copies
Sent to :	Jérôme Benveniste Marco Restano	ESA SERCO/ESRIN	1 (digital copy)
Internal copy :	Project Report	Magellium	1 (digital copy)

Document evolution sheet

Ed.	Rev.	Date	Purpose evolution	Comments
1	0	02/02/2022	Creation of document	
1	1	15/06/2022	Minor modifications due to ESA feedbacks	
1	2	17/08/2022	Minor modifications	Introduction section 2 - Sections 2.1, 3.5.2, 4.4.6, 5.4.3

Contents

1. Introduction	7
1.1. Executive summary	7
1.2. Scope and objectives	7
1.3. Document structure	8
1.4. Related documents	8
1.5.1. Applicable documents	8
1.5.2. Reference documents	9
1.5. Terminology	10
1.6. References	11
2. Physical principle	13
2.1. The (Integrated) Expansion Efficiency of Heat	13
2.2. OHC change calculation	13
2.3. Comments	14
2.3.1. Temporal reference of the TSSL	14
2.3.2. Time derivative of the OHC change	15
3. Input data	15
3.1. Overview	15
3.2. Ocean mass	15
3.2.1. Description	15
3.2.2. Comments/limitations	16
3.3. Sea level	17
3.3.1. Description	17
3.3.2. Comments/limitations	17
3.3.3. Specific corrections	17
3.4. Halosteric sea level	19
3.4.1. Description	19
3.4.2. Comments/limitations	20
3.5. Integrated Expansion Efficiency of Heat	20
3.5.1. Description	20
3.5.2. Regional estimates of the integrated EEH	20
3.5.3. Comments/limitations	22
3.6. Static data: water ratio	23
3.7. Static data: grid cells area	23
4. 4DAtlantic OHC processing chain	23

4.1. Outline	23
4.2. Input data	24
4.3. Output data	24
4.4. Retrieval methodology	25
4.4.1. Overview	25
4.4.2. Preprocessing of SL change grids	25
4.4.2.1. Description	25
4.4.2.2. Mathematical statement	25
Temporal interpolation	25
Spatial filtering	25
Spatial interpolation	26
Corrections applied	26
4.4.2.3. Comments/limitations	26
4.4.3. Preprocessing of OM change grids	26
4.4.3.1. Description	26
4.4.3.2. Mathematical statement	26
Management of the data gap	27
Addition of a high frequency component into the data gaps	27
4.4.3.3. Comments/limitations	27
4.4.4. Preprocessing of HSSL change grids	27
4.4.4.1. Description	28
4.4.5. Calculation of regional TSSL change grids	28
4.4.5.1. Description	28
4.4.5.2. Mathematical statement	28
4.4.5.3. Comments/limitations	28
4.4.6. Calculation of regional OHC change grids	29
4.4.6.1. Description	29
4.4.6.2. Mathematical statement	29
4.4.6.3. Comments/limitations	29
5. Uncertainties calculation and propagation	29
5.1. Overview	30
5.2. Input Data	31
5.3. Output Data	32
5.4. Retrieval methodology	32
5.4.1. Calculation of the SL covariance matrix	32
5.4.1.1. Description	32
5.4.1.2. Mathematical statement	32

5.4.1.3. Comments/Limitations	33
5.4.2. Calculation of the OM covariance matrix	33
5.4.2.1. Description	33
5.4.2.2. Mathematical statement	33
5.4.2.3. Comments/Limitations	33
5.4.3. Calculation of the HSSL covariance matrix	34
5.4.4. Calculation of the TSSL covariance matrix	34
5.4.4.1. Description	34
5.4.4.2. Mathematical statement	34
5.4.4.3. Comments/Limitations	34
5.4.5. Calculation of the OHC covariance matrix	35
5.4.5.1. Description	35
5.4.5.2. Mathematical statement	35
5.4.5.3. Uncertainties of the regional IEEH	36
5.4.5.4. Comments/Limitations	36
5.4.6. Calculation of trend uncertainties	36
5.4.6.1. Description	36
5.4.6.2. Mathematical statement	37
5.4.6.3. Comments/Limitations	37

List of figures

Figure 1: 4DAtlantic processing chain steps for the estimation of OHC change and its uncertainties	8
Figure 2: diagram of OHC change and its time derivative calculation with IEEH approach	13
Figure 3: Regional grid of the GIA correction applied to altimetry sea level grids in 4DAtlantic processing chain (Spada and Melini, 2019)	18
Figure 4: Time-mean of the Integrated Expansion Efficiency of Heat (IEEH) coefficients (10-21 m/J) (1x1 degree).	22
Figure 5: Overview of the 4DAtlantic processing chain. Variables are given with their dimensions (lon: longitude, lat: latitude, t: time)	24
Figure 6: Uncertainty calculation and propagation chain	31

List of tables

Table 1: List of reference documents	9
Table 2: List of abbreviations and acronyms	10
Table 3: Altimetry regional error budget given at 1-sigma	32

1. Introduction

1.1. Executive summary

Given the major role of the Atlantic Ocean in the climate system, it is essential to characterise the temporal and spatial variations of its heat content. The 4DAtlantic Project (<https://eo4society.esa.int/projects/4datlantic-ohc/>) aims at developing and testing space geodetic methods to estimate the regional **ocean heat content** (OHC) change over the Atlantic Ocean from satellite altimetry and gravimetry. The strategy developed in the frame of the ESA MOHeaCAN Project (<https://eo4society.esa.int/projects/moheacan/>) is pursued and refined at spatial regional scales both for the data generation and the uncertainty estimate. At two test sites, OHC change derived from in situ data (RAPID and OVIDE-AR7W) are used to evaluate the accuracy and reliability of the new space geodetic based OHC change. The Atlantic OHC product will be used to better understand the complexity of the Earth's climate system. In particular, the project aims at better understanding the role played by the Atlantic Meridional Overturning Circulation (AMOC) in regional and global climate change, and the variability of the Meridional Heat transport in the North Atlantic. In addition, improving our knowledge on the Atlantic OHC change will help to better assess the global ocean heat uptake and thus estimate the Earth's energy imbalance more accurately as the ocean absorbs about 90% of the excess energy stored by the Earth system.

In the 4DAtlantic project, the OHC change is estimated from the measurement of the thermal expansion of the ocean. The latter is obtained by removing the ocean mass change and the sea level change due to salinity (halosteric sea level changes) derived from gravimetry and in situ data respectively to the total sea-level change derived from altimetry measurements. This approach provides consistent spatial and temporal sampling of the ocean heat content change in the Atlantic Ocean.

4DAtlantic project's objectives are to develop novel algorithms, estimate realistic regional OHC uncertainties thanks to a rigorous error budget of the altimetric, gravimetric and in-situ instruments in order to reach the challenging target for the uncertainty quantification.

1.2. Scope and objectives

This document is the Algorithm Theoretical Basis Document (ATBD) of the 4DAtlantic OHC product supported by ESA. This ATBD is dedicated to the description and justification of the algorithms used in the generation of the **OHC change**.

The calculation of the 4DAtlantic OHC product is divided in several steps as presented in the following figure (Figure 1). The first step is to process the input data from the altimetry, gravimetry and in-situ measurements to allow their differences to be calculated in the next step. Then the processing of the OHC at spatial regional scales can be carried out. The last step consists in computing uncertainties of the 4DAtlantic OHC product, propagating the uncertainties at spatial regional scales from input data until the final product.

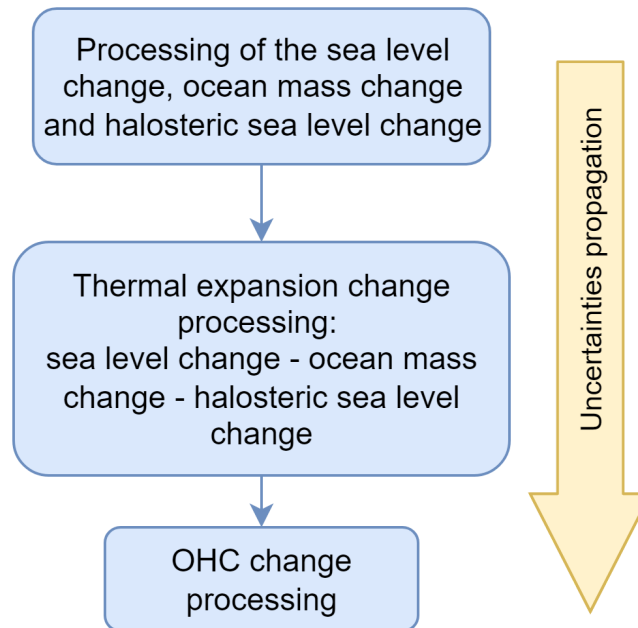


Figure 1: 4DAtlantic processing chain steps for the estimation of OHC change and its uncertainties

This ATBD is divided into 4 sections. We first give a brief summary of the method, then we describe the input data for the processing chain, mainly altimetry, gravimetry and in-situ observations. We then explain how the OHC change is calculated at spatial regional scale before presenting the uncertainty propagation methodology in the last section.

1.3. Document structure

In addition to this introduction, the document is organised as follows:

- Section 2 explains the physical principle of the space geodetic approach and OHC change calculation
- Section 3 provides the description of the input data of the 4DAtlantic processing chain.
- Section 4 provides a detailed description and justification of every step in the OHC computation.
- Section 5 provides a detailed description and justification of the uncertainty propagation methodology until the final OHC product.

1.4. Related documents

1.5.1. Applicable documents

The following table lists the documents with a direct bearing on the content of this document.

Id.	Reference	Name of Document
AD1	OHCATL-DT-035-MAG_Experimental_Dataset_Description	Experimental Dataset Description (EDD) - 4DAtlantic OHC product user manual

Table 1: List of applicable documents

1.5.2. Reference documents

The following table lists the materials which contain information in support of this document.

Id.	Ref.	Description
RD1	-	C3S data store: https://cds.climate.copernicus.eu/
RD2	D3.SL.1-v2.0_PUGS_of_v2DT2021_SeaLevel_products_v1.1_APPROVED_Ver1.pdf	Product product user manual of sea level daily gridded data for the global ocean from 1993 to present from Copernicus Climate Change Service (C3S): https://datastore.copernicus-climate.eu/documents/satellite-sea-level/vDT2021/D3.SL.1-v2.0_PUGS_of_v2DT2021_SeaLevel_products_v1.1_APPROVED_Ver1.pdf
RD3	D1.SL.2-v2.0_ATBD_of_v2DT2021_SeaLevel_products_v1.1_APPROVED_Ver1.pdf	Algorithm Theoretical Basis Document of sea level daily gridded data for the global ocean from 1993 to present from Copernicus Climate Change Service (C3S): https://datastore.copernicus-climate.eu/documents/satellite-sea-level/vDT2021/D1.SL.2-v2.0_ATBD_of_v2DT2021_SeaLevel_products_v1.1_APPROVED_Ver1.pdf
RD4	ftp://ftp.legos.obs-mip.fr/pub/soa/gravimetrie/grace/legos/V1.5.1/	Ensemble of the ocean mass solutions provided by Blazquez et al., (2018) on LEGOS FTP site.
RD5	https://grace.jpl.nasa.gov/data/data-updates/	Jet Propulsion Laboratory (NASA) website dedicated to Gravity recovery and climate experiment, GRACE and GRACE-FO missions.
RD6	https://www.seanoe.org/data/00412/52367/	Sea scientific open data edition (SEANOE) website dedicated to ISAS20 temperature and salinity gridded fields
RD7	https://www.metoffice.gov.uk/hadobs/en4/download-en4-2-2.html	Met Office Hadley Center website dedicated to EN4.2.2.I09 temperature and salinity gridded fields

Table 2: List of reference documents

1.5. Terminology

Abbreviation/acronym	Description
AMOC	Atlantic Meridional Overturning Circulation
ATBD	Algorithm theoretical basis document
Argo	International program that uses profiling floats deployed worldwide to observe ocean properties such as temperature and salinity.
C3S	Copernicus Climate Change Service
COST-G	International Combination Service for Time-variable Gravity Fields
EDD	Experimental dataset description
EEH	Expansion efficiency of heat
ESA	European Space Agency
EWH	Equivalent water height
FTP	File transfer protocol
GFZ	Deutsches GeoForschungsZentrum or German research center for geosciences
GIA	Glacial isostatic adjustment
GMWTC	Global mean wet tropospheric correction
GRACE(-FO)	Gravity recovery and climate experiment (-Follow on)
GRD	Changes in Earth Gravity, Earth Rotation and viscoelastic solid-Earth Deformation
GSFC	Goddard Space Flight Center
HSSL	Halosteric sea level
IEEH	Integrated expansion efficiency of heat
JPL	Nasa's jet propulsion laboratory
LEGOS	Laboratoire d'Etudes en Géophysique et Océanographie Spatiale
MSS	Mean sea surface
MWR	Microwave radiometer
OHC	Ocean heat content
OHU	Ocean heat uptake
OLS	Ordinary least square
OM	Ocean mass
RD	Reference document
SL	Sea level
SLA	Sea level anomaly

SSL	Steric sea level
TSSL	Thermosteric sea level
TUG	Technische Universität Graz or Technical university of Graz

Table 3: List of abbreviations and acronyms

1.6. References

- Ablain, M., Cazenave, A., Larnicol, G., Balmaseda, M., Cipollini, P., Faugère, Y., Fernandes, M. J., Henry, O., Johannessen, J. A., Knudsen, P., Andersen, O., Legeais, J., Meyssignac, B., Picot, N., Roca, M., Rudenko, S., Scharffenberg, M. G., Stammer, D., Timms, G., and Benveniste, J.: Improved sea level record over the satellite altimetry era (1993–2010) from the Climate Change Initiative project, *Ocean Sci.*, 11, 67–82, <https://doi.org/10.5194/os-11-67-2015>, 2015.
- Ablain, M., Meyssignac, B., Zawadzki, L., Jugier, R., Ribes, A., Spada, G., Benveniste, J., Cazenave, A., and Picot, N.: Uncertainty in satellite estimates of global mean sea-level changes, trend and acceleration, *Earth Syst. Sci. Data*, 11, 1189–1202, <https://doi.org/10.5194/essd-11-1189-2019>, 2019.
- Barnoud, A., Pfeffer, J., Guérou, A., Frery, M.-L., Siméon, M., Cazenave, A., Chen, J., Llovel, W., Thierry, V., Legeais, J.-F., and Ablain, M.: Contributions of altimetry and Argo to non-closure of the global mean sea level budget since 2016, *Geophys. Res. Lett.*, <https://doi.org/10.1029/2021gl092824>, 2021.
- Barnoud, A., Picard, B., Meyssignac, B., Marti, F., Ablain, M., and Roca, R.: Reducing the long term uncertainties of global mean sea level using highly stable water vapour climate data records, in revision.
- Barnoud, A., Pfeffer, J., Cazenave, A., and Ablain, M.: Revisiting the global ocean mass budget over 2005-2020, in prep.
- Blazquez, A., Meyssignac, B., Lemoine, J., Berthier, E., Ribes, A., and Cazenave, A.: Exploring the uncertainty in GRACE estimates of the mass redistributions at the Earth surface: implications for the global water and sea level budgets, *Geophys. J. Int.*, 215, 415–430, <https://doi.org/10.1093/gji/ggy293>, 2018.
- Carrère, L. and Lyard, F.: Modeling the barotropic response of the global ocean to atmospheric wind and pressure forcing - comparisons with observations, *Geophys. Res. Lett.*, 30, 1275, <https://doi.org/10.1029/2002GL016473>, 2003.
- Frederikse, T., Riva, R. E. M., and King, M. A.: Ocean Bottom Deformation Due To Present-Day Mass Redistribution and Its Impact on Sea Level Observations, *Geophys. Res. Lett.*, 44, 12,306-12,314, <https://doi.org/10.1002/2017GL075419>, 2017.
- Gaillard, F., Reynaud, T., Thierry, V., Kolodziejczyk, N., and Schuckmann, K. von: In Situ-Based Reanalysis of the Global Ocean Temperature and Salinity with ISAS: Variability of the Heat Content and Steric Height, *J. Clim.*, 29, 1305–1323, <https://doi.org/10.1175/JCLI-D-15-0028.1>, 2016.
- Good, S. A., Martin, M. J., and Rayner, N. A.: EN4: Quality controlled ocean temperature and salinity profiles and monthly objective analyses with uncertainty estimates, *J. Geophys. Res. Oceans*, 118, 6704–6716, <https://doi.org/10.1002/2013JC009067>, 2013.
- Kuhlbrodt, T. and Gregory, J. M.: Ocean heat uptake and its consequences for the magnitude of sea level rise and climate change, *Geophys. Res. Lett.*, 39, <https://doi.org/10.1029/2012GL052952>, 2012.
- Legeais, J.-F., Meyssignac, B., Faugère, Y., Guérou, A., Ablain, M., Pujol, M.-I., Dufau, C.,

- and Dibarboure, G.: Copernicus Sea Level Space Observations: A Basis for Assessing Mitigation and Developing Adaptation Strategies to Sea Level Rise, *Front. Mar. Sci.*, 8, 2021.
- Levitus, S., Antonov, J. I., Boyer, T. P., Baranova, O. K., Garcia, H. E., Locarnini, R. A., Mishonov, A. V., Reagan, J. R., Seidov, D., Yarosh, E. S., and Zweng, M. M.: World ocean heat content and thermosteric sea level change (0–2000 m), 1955–2010, *Geophys. Res. Lett.*, 39, <https://doi.org/10.1029/2012GL051106>, 2012.
 - Marti, F., Blazquez, A., Meyssignac, B., Ablain, M., Barnoud, A., Fraudeau, R., Jugier, R., Chenal, J., Larnicol, G., Pfeffer, J., Restano, M., and Benveniste, J.: Monitoring the ocean heat content change and the Earth energy imbalance from space altimetry and space gravimetry, *Earth Syst. Sci. Data*, <https://doi.org/10.5194/essd-2021-220>, 2022.
 - McDougall, T. J. and Barker, P. M.: Getting started with TEOS-10 and the Gibbs Seawater (GSW) Oceanographic Toolbox, 2011.
 - Meyssignac, B., Boyer, T., Zhao, Z., Hakuba, M. Z., Landerer, F. W., Stammer, D., Köhl, A., Kato, S., L’Ecuyer, T., Ablain, M., Abraham, J. P., Blazquez, A., Cazenave, A., Church, J. A., Cowley, R., Cheng, L., Domingues, C. M., Giglio, D., Gouretski, V., Ishii, M., Johnson, G. C., Killick, R. E., Legler, D., Llovel, W., Lyman, J., Palmer, M. D., Piotrowicz, S., Purkey, S. G., Roemmich, D., Roca, R., Savita, A., Schuckmann, K. von, Speich, S., Stephens, G., Wang, G., Wijffels, S. E., and Zilberman, N.: Measuring Global Ocean Heat Content to Estimate the Earth Energy Imbalance, *Front. Mar. Sci.*, 6, <https://doi.org/10.3389/fmars.2019.00432>, 2019.
 - Palmer, M. D. and McNeall, D. J.: Internal variability of Earth’s energy budget simulated by CMIP5 climate models, *Environ. Res. Lett.*, 9, 034016, <https://doi.org/10.1088/1748-9326/9/3/034016>, 2014.
 - Prandi, P., Meyssignac, B., Ablain, M., Spada, G., Ribes, A., and Benveniste, J.: Local sea level trends, accelerations and uncertainties over 1993–2019, *Sci. Data*, 8, 1, <https://doi.org/10.1038/s41597-020-00786-7>, 2021.
 - Russell, G. L., Gornitz, V., and Miller, J. R.: Regional sea level changes projected by the NASA/GISS Atmosphere-Ocean Model, *Clim. Dyn.*, 16, 789–797, <https://doi.org/10.1007/s003820000090>, 2000.
 - Spada, G. and Melini, D.: On Some Properties of the Glacial Isostatic Adjustment Fingerprints, *Water*, 11, 1844, <https://doi.org/10.3390/w11091844>, 2019.
 - Taylor, J. R.: An Introduction to Error Analysis: The Study of Uncertainties in Physical Measurements, 2nd ed., University Science Books, Sausalito, California, 344 pp., 1997.
 - Wahr, J., Swenson, S., Zlotnicki, V., and Velicogna, I.: Time-variable gravity from GRACE: First results: TIME-VARIABLE GRAVITY FROM GRACE, *Geophys. Res. Lett.*, 31, n/a-n/a, <https://doi.org/10.1029/2004GL019779>, 2004.
 - WCRP Global Sea Level Budget Group: Global sea-level budget 1993–present, *Earth Syst. Sci. Data*, 10, 1551–1590, <https://doi.org/10.5194/essd-10-1551-2018>, 2018.
 - Wong, A. P. S., Wijffels, S. E., Riser, S. C., Pouliquen, S., Hosoda, S., Roemmich, D., Gilson, J., Johnson, G. C., Martini, K., Murphy, D. J., Scanderbeg, M., Bhaskar, T. V. S. U., Buck, J. J. H., Merceur, F., Carval, T., Maze, G., Cabanes, C., André, X., Poffa, N., Yashayaev, I., Barker, P. M., Guinehut, S., Belbéoch, M., Ignaszewski, M., Baringer, M. O., Schmid, C., Lyman, J. M., McTaggart, K. E., Purkey, S. G., Zilberman, N., Alkire, M. B., Swift, D., Owens, W. B., Jayne, S. R., Hersh, C., Robbins, P., West-Mack, D., Bahr, F., Yoshida, S., Sutton, P. J. H., Cancouët, R., Coatanoan, C., Dobbler, D., Juan, A. G., Gourrion, J., Kolodziejczyk, N., Bernard, V., Bourlès, B., Claustre, H., D’Ortenzio, F., Le Reste, S., Le Traon, P.-Y., Rannou, J.-P., Saout-Grit, C., Speich, S., Thierry, V., Verbrugge, N., Angel-Benavides, I. M., Klein, B., Notarstefano, G., Poulain, P.-M., Vélez-Belchí, P., Suga, T., Ando, K., Iwasaska, N., Kobayashi, T., Masuda, S., Oka, E., Sato, K., Nakamura, T., Sato, K., Takatsuki, Y., Yoshida, T., Cowley, R., Lovell, J. L., Oke,

P. R., van Wijk, E. M., Carse, F., Donnelly, M., Gould, W. J., Gowers, K., King, B. A., Loch, S. G., Mowat, M., Turton, J., Rama Rao, E. P., Ravichandran, M., Freeland, H. J., Gaboury, I., Gilbert, D., Greenan, B. J. W., Ouellet, M., Ross, T., Tran, A., Dong, M., Liu, Z., Xu, J., Kang, K., Jo, H., et al.: Argo Data 1999–2019: Two Million Temperature-Salinity Profiles and Subsurface Velocity Observations From a Global Array of Profiling Floats, *Front. Mar. Sci.*, 7, 2020.

2. Physical principle

In the framework of the 4DAtlantic-OHC project, the regional **OHC change** is calculated from the **ThermoStereic Sea Level (TSSL) change** with satellite data. For this purpose, a coefficient of expansion efficiency of heat is needed to do the conversion of thermal expansion into OHC change.

In this document, the word “change” refers to the difference between any two states - it refers to the difference between the present state (t) and the state to a given date (t_{ref}) or time period.

2.1. The (Integrated) Expansion Efficiency of Heat

The expansion efficiency of heat (EEH) expresses the change in ocean density due to heat uptake. As a matter of fact it represents the ratio of the temporal derivative of thermosteric sea level over the temporal derivative of the heat content under a given heat uptake. The EEH is dependent on temperature, salinity and pressure (Russell et al., 2000). Thus, integrated over the total water column, the EEH is supposed to vary with latitude along with the variations of integrated salinity, temperature and pressure. At a regional scale, the EEH has never been calculated. To explain this, it occurs that the OHC change over an entire water column can be null whilst the thermosteric component of the SSL change is not. In such a situation, the EEH is not defined and cannot be calculated. A way to avoid this issue is to consider the **integrated expansion efficiency of heat (IEEH)** instead of the EEH (Marti et al., 2022). In the 4DAtlantic project, the IEEH approach is chosen and allows the conversion of thermal expansion derived from the ThermoStereic sea Level (TSSL) change into OHC change. This IEEH coefficient can be retrieved from in-situ measurements. More explanations on the methodology to compute the IEEH coefficient are given in section [3.5](#).

2.2. OHC change calculation

The diagram below presents the relationship between the main variables that are used to calculate the Ocean Heat Content (OHC) change and its time derivative from the TSSL change (obtained from removing the HaloStereic Sea Level (HSSL) change and the Ocean Mass (OM) change to the total Sea-Level (SL) change) and applying the Integrated Expansion Efficiency of Heat (IEEH) coefficient.

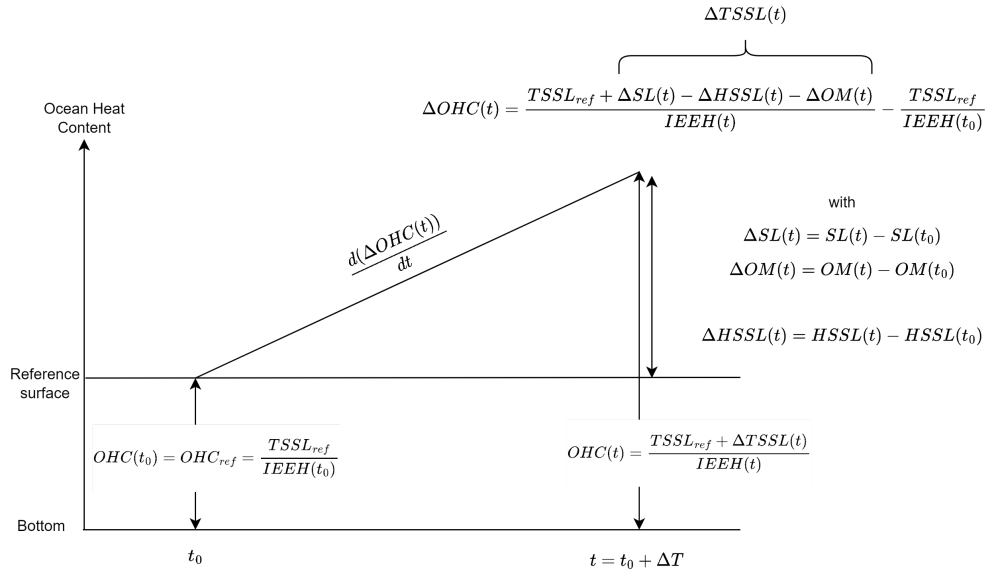


Figure 2: diagram of OHC change and its time derivative calculation with IEEH approach

OHC change ($\Delta OHC(t)$) is defined by the difference between OHC at t and t_0 , and can be written as follow:

$$\Delta OHC(t) = \frac{TSSL_{ref} + \Delta TSSL(t)}{IEEH(t)} - \frac{TSSL_{ref}}{IEEH(t_0)} \quad \text{Eq. 1}$$

Where $\Delta TSSL$ is the TSSL change, $IEEH$ the integrated expansion efficiency of heat and $TSSL_{ref}$ is the reference of the TSSL at $t = t_0$.

2.3. Comments

2.3.1. Temporal reference of the TSSL

As TSSL change is calculated from SL, OM and HSSL change (Equation 2), it is important to note that all these parameters have their own reference. If we consider that they have the same reference (i.e. they are all null at $t = t_0$) we have the following equation:

$$\Delta_{t_0} TSSL(t) = \Delta_{t_0} SL(t) - \Delta_{t_0} OM(t) - \Delta_{t_0} HSSL(t) \quad \text{Eq. 2}$$

However, in practice, SL, OM and HSSL change (see section 3.) are not referenced at the same time or period. If we consider that OM, SL and HSSL change are respectively referenced at

$t = t_1$, $t = t_2$ and $t = t_3$ and that the goal is to reference the TSSL change at $t = t_0$, we have to compute the following equation for the TSSL change calculation:

$$\Delta_{t_0} TSSL(t) = \Delta_{t_1} SL(t) - \Delta_{t_2} OM(t) - \Delta_{t_3} HSSL(t) - (\Delta_{t_1} SL(t_0) - \Delta_{t_2} OM(t_0) - \Delta_{t_3} HSSL(t_0)) \quad \text{Eq. 3}$$

With this calculation, we get by construction the TSSL change and the OHC change at t_0 equal to 0 whatever the time reference of SL, OM and HSSL change.

2.3.2. Time derivative of the OHC change

The time derivative of the OHC change is written as:

$$\frac{d(\Delta OHC(t))}{dt} = \frac{d}{dt} \left(\frac{TSSL_{ref}}{IEEH(t)} \right) + \frac{d}{dt} \left(\frac{\Delta TSSL(t)}{IEEH(t)} \right) \quad \text{Eq. 4}$$

It is important to note that $TSSL_{ref}$ is important for the calculation of the time derivative of the OHC change. The choice of this reference will be further given in the section [4.4.6.](#)

3. Input data

3.1. Overview

The following section describes the different datasets used for the computation of the OHC change grids. They include time-varying data such as the total SL change, the HSSL change, the OM change and the integrated expansion efficiency of heat, which is used to convert thermal expansion change into ocean heat content change. There is also static data such as the water ratio, grid cells area and the Glacial Isostatic Adjustment. These inputs are spatial data given on the entire globe. However, their spatial availability is different and may vary over time. The origin and format of each dataset are described in a dedicated subsection. The limitations and errors associated with the dynamic input datasets are also presented.

3.2. Ocean mass

3.2.1. Description

Ocean mass (OM) change estimates are derived from gravimetric measurements. GRACE and GRACE Follow On (GRACE-FO) missions provide the Earth's surface mass changes from 04/2002 to 09/2021 [[RD5](#)]. As GRACE data are impacted by different error sources (Blazquez

et al., 2018; Meyssignac et al., 2019), we used an ensemble approach in order to average the errors and also to evaluate the uncertainty in ocean mass.

Blazquez et al. (2018) provided an ensemble of OM solutions derived from GRACE. Spherical harmonics solutions from various processing centers have been considered as those from the Center for Space Research (CSR), the Jet Propulsion laboratory (JPL), the Deutsches GeoForschungsZentrum (GFZ), the Technische Universität Graz (TUG), the Groupe de Recherche en Géodésie Spatiale (GRGS), and the International Combination Service for Time-variable Gravity Fields (COST-G). These solutions cannot be directly used to estimate the ocean mass; they need first to be post-processed (Wahr et al., 2004). The post-processing parameters includes (i) the addition of independent estimates of the degree 1 and degree 2 order 0 spherical harmonics (as these harmonics are not observable by GRACE), (ii) a filtering for correlated errors that maps into characteristic north-south stripes, (iii) a correction for the large land signals (from hydrology or glaciers) that can 'leak' into the ocean because of the limited spatial resolution of GRACE, and (iv) a correction for glacial isostatic adjustment (GIA). Blazquez et al. (2018) applied a range of state-of-the-art post-processing parameters to get a spread of GRACE estimates of the ocean mass. A time mean over 2005–2015 is removed from all GRACE solutions to compute anomalies.

For this study we used an update of the ensemble from Blazquez et al. (2018), including the GRACE-FO mission and considering datasets from different processing centers and different post-processing parameters, including an earthquake correction. The version v1.5.1 that is used includes new improvements. In comparison with the v1.5 version, we note:

- Increase of the temporal coverage and reduction of data gap between GRACE and GRACE-FO (gap is now from 06/2017 to 07/2018)
- Regional ocean mass change derived from GRACE/GRACE-FO further than 300 km is used to correct the first 300 km near Greenland and Antarctica
- New Geocenter products taken into account.

This led to a new ensemble of 288 solutions.

OM data is described and available in NetCDF format file on the following LEGOS FTP [Table 2, [RD4](#)]. Its content is described below:

- Ensemble of 288 OM solutions and its ensemble mean (Blazquez et al., 2018)
 - units: m equivalent water height (EWH)
 - spatial resolution: $1^\circ \times 1^\circ$
 - temporal resolution: monthly
 - temporal availability: April 2002 - September 2021
 - version: v1.5.1

3.2.2. Comments/limitations

As explained in Blazquez et al. (2018), the combination of the different raw solutions (from processing centers) with the different post-processing parameters (geocenter motion correction, filtering techniques, leakage and GIA corrections) leads to an ensemble which is assumed to cover a significant part of the uncertainty range of GRACE/GRACE-FO ocean mass estimates.

For this reason, the entire 288 solutions ensemble is used to estimate the OM change uncertainties at regional scale (see section [5.4.2.](#)).

3.3. Sea level

3.3.1. Description

Sea level change at regional scales are derived from the sea-level products operationally generated by the Copernicus Climate Change Service (C3S). This dataset, fully described in (Legeais et al., 2021) is dedicated to the sea level stability for climate applications. It provides daily sea-level anomalies grids based at any time on a reference altimeter mission (TopEx/Poseidon, Jason-1,2,3 and S6-MF very soon) plus complementary missions (ERS-1,2, Envisat, Cryosat, SARAL/Altika, Sentinel-3A) to increase spatial coverage.

C3S provides the sea level anomaly (SLA) around a mean sea surface (MSS) above the reference mean sea-surface computed over 1993-2012, or in other words, the total SL change [Table 2, [RD2](#)]. Data is available in NetCDF format files on the C3S data store [Table 2, [RD1](#)]. The main characteristics of SLA grids are:

- spatial resolution: $0.25^\circ \times 0.25^\circ$
- temporal resolution: daily
- temporal availability: altimetry era, January 1993 - August 2021
- units: m
- version: vDT2021

More information is available in the product user manual of C3S [[RD2](#)] and the algorithm description document [[RD3](#)].

3.3.2. Comments/limitations

C3S data result from the most up-to-date standards (altimeter standards, geophysical corrections) whose timeliness is compatible with the C3S production planning and most of them follow the recommendations of the ESA Sea Level CCI project. They are submitted to a rigorous validation process.

However, these data are affected by errors like any spatial measurements. The full description of these errors was already described at global scale (Ablain et al., 2015, 2019). In a further study, a full estimation of the regional altimetry error budget was used to derive regional error variance-covariance matrices (Prandi et al., 2021). These error matrices are well adapted to the description of C3S data measurements because the SL errors are the same (similar altimeter standards). It has therefore been used as an input for the error propagation purpose in this project (see section [5](#). devoted to this topic).

3.3.3. Specific corrections

Grids of sea level change provided by C3S do not take in consideration the global isostatic adjustment (GIA) process in response to the melting of the Late Pleistocene ice sheets. However, this effect needs to be corrected in sea level change estimates as it does not reflect the ocean's response to recent climate change. GIA contains regional variations that must be

corrected. It is still an area of active research, and then several GIA grids expressed as trends in lithospheric height change (in mm/year) are available in the literature. The same GIA correction used in the recent study (Prandi et al., 2021) for an estimation of the sea level trends uncertainties at regional scale has been applied. It is an ensemble mean of the regional GIA results for model ICE-5G, with various viscosity profiles (27 profiles). The methodology is also described in (Spada and Melini, 2019). The average GIA value over oceans from this 27 solution ensemble is $0,33 \text{ mm.yr}^{-1}$ closely matching the value of -0.3 mm.yr^{-1} (WCRP Global Sea Level Budget Group, 2018), generally adopted as a rule of thumb to correct the altimetric absolute sea-level trend for the effects of past GIA.

An additional correction is considered to take into account the ocean bottom deformation due to present-day mass redistribution. This correction GRD (changes in Earth Gravity, Earth Rotation and viscoelastic solid-Earth Deformation) has been evaluated at 0.1 mm/yr during the altimetry area (1993-2014), (Frederikse et al., 2017). We have applied this correction only on sea level observations because this effect has no impact on the gravimetric data. The constant value is used in the regional computation.

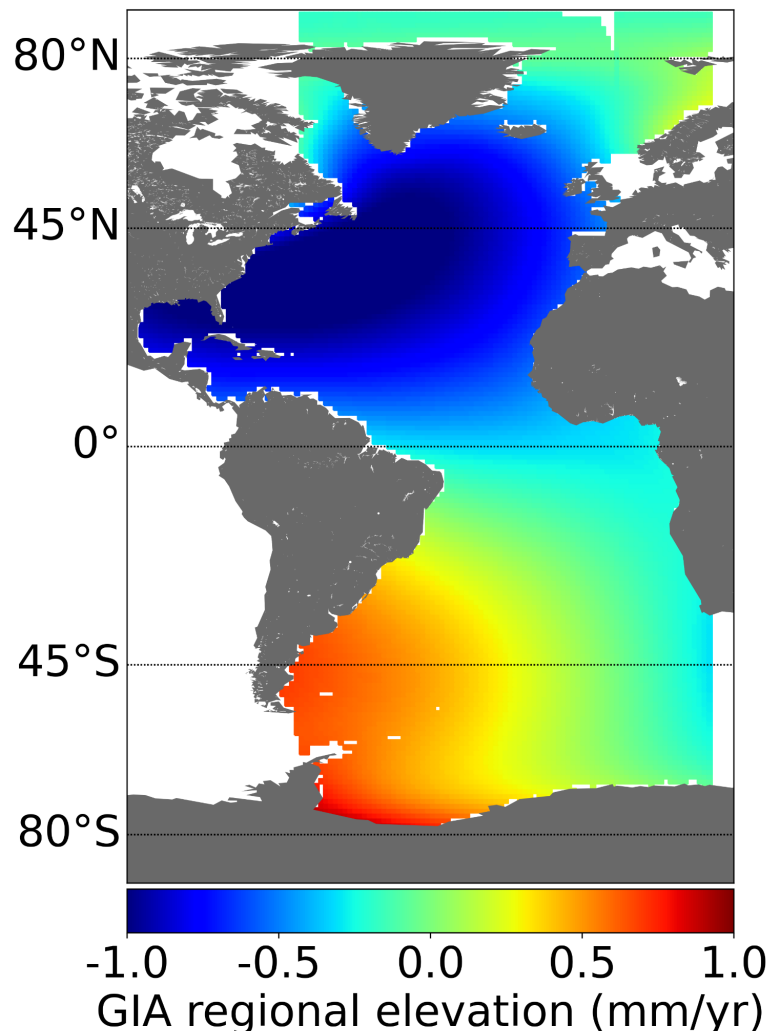


Figure 3: Regional grid of the GIA correction applied to altimetry sea level grids in 4DAtlantic processing chain (Spada and Melini, 2019)

Moreover, recent studies have shown that a drift on Jason-3 radiometer has been detected and a correction should be applied on sea level grids. This correction was calculated from the relative differences between the global mean wet tropospheric correction (GMWTC) from Jason-3 microwave radiometer (MWR) and the GMWTC derived from water vapour climate data records (Barnoud et al., in revision), the GMWTC from SARAL/AltiKa's MWR and the GMWTC from Sentinel-3A. The correction C_{J3} is computed as the average of the zero-mean GMWTC differences (Barnoud et al., in prep.).

3.4. Halosteric sea level

3.4.1. Description

The halosteric sea level (HSSL) change is estimated from in situ data of temperature (T) and salinity (S) depending on time, latitude, longitude and depth. These allow to compute the sea level height change due to salinity change $\Delta HSSL_{h_i}$ for a given layer of the water column h_i . For a given time, latitude and longitude, $\Delta HSSL$ is obtained as the integration of the $\Delta HSSL_{\Delta h_i}$ over the vertical following the equation:

$$\Delta HSSL(t, lat, lon) = \sum_i \Delta HSSL_{h_i}(t, lat, lon) = \sum_i \frac{(\rho_{ref} - \rho(T_{clim}, S, \Sigma_i h_i)) \cdot |h_i|}{\rho_{ref}}(t, lat, lon) \quad \text{Eq. 5}$$

Where

- h_i is the i-th value of the thickness layer so that $\sum_i h_i$ is the depth of integration (in m),
- ρ_{ref} is the reference value of the density computed at fixed Salinity (35psu) and Temperature (0°C),
- $\rho(T_{clim}, S, \Sigma_i h_i)$ is the density with temperature fixed at the climatology

The HSSL change is thus obtained with the following equation. For the 4DAtlantic product, the computation relies on the thermodynamic equation of seawater (McDougall and Barker, 2011) and the period 2005-2015 is used for the climatology. The HSSL component is estimated from the combination of two in situ temperature and salinity datasets. From 0m to 2000m depth, the HSSL is calculated by using ISAS20 temperature and salinity datasets [RD6]. Between 2000m and 6000m, HSSL is calculated based upon EN4.2.2.109 temperature and salinity gridded fields [RD7]. ISAS20 temperature and salinity is given at a 0.5° x 0.5° resolution whereas EN4.2.2.109 is given at a 1°x1° resolution. Before making the sum of both HSSL contributions, the HSSL based upon ISAS20 is first interpolated at a 1°x1° resolution.

The main characteristics of HSSL change grids are:

- spatial resolution: 1° x 1°
- temporal resolution: monthly
- depth integration: 0-6000m (IFREMER ISAS20 from 0 to2000m & EN4.2.2.I09 2000m to 6000m)
- temporal availability: January 2002 - December 2020
- units: m

3.4.2. Comments/limitations

ISAS20 represents the most recent standard dataset for temperature and salinity from IFREMER. The ISAS procedure and product is described in Gaillard et al. (2016). The ISAS20 product is based on the measurements from the Argo and Deep Argo floats.

EN4.2.2.I09 product from Met Office has been chosen to address the deep ocean contribution as it is known to have the most important sources of deep ocean information such as XBT, CTD and MBT profiles (Good et al., 2013). Even if it appears to be the best product to use at the time of writing. Note that all those measurements performed in the deep ocean layers remain sporadic both spatially and across time and that most of the deep ocean signal is close to the climatology.

Recent studies highlight that in situ salinity datasets from Argo present a drift from 2016 due to anomalies on the conductivity sensors (Wong et al., 2020). Barnoud et al. (2021) showed that this affects the HSSL estimates. The impact of this halosteric drift from in situ measurements has not been quantified yet on the 4DAtlantic OHC product.

3.5. Integrated Expansion Efficiency of Heat

3.5.1. Description

The integrated expansion efficiency of heat (IEEH) expresses the ratio between the thermosteric sea level change and the ocean heat content change.

3.5.2. Regional estimates of the integrated EEH

In the framework of this project, IEEH values are provided at spatial regional scales and at a 1-degree resolution 3D monthly grid, calculated based on in situ temperature and salinity fields. IEEH is defined as the ratio between TSSL change and OHC change:

$$IEEH(t, lat, lon) = \frac{\Delta TSSL(t, lat, lon)}{\Delta OHC(t, lat, lon)} \quad \text{Eq. 6}$$

where :

- $\Delta TSSL(t, lat, lon)$ is the thermosteric sea-level change referenced to a physical thermosteric sea-level content (defined at 0° Celsius and 35 PSU) and calculated from in-situ measurements of temperature and salinity following :

$$\Delta TSSL(t, lat, lon) = [\sum_j \frac{(\rho_{ref} - \rho(T, S_{clim}, \Sigma_i h_i)) \cdot |h_j|}{\rho_{ref}}](t, lat, lon) \quad \text{Eq. 7}$$

- $\Delta OHC(t, lat, lon)$ is the ocean heat content change integrated over the whole water column and is calculated following the equation :

$$\Delta OHC(t, lat, lon) = [\sum_j \rho(T, S, \Sigma_i h_i) \cdot C_p(T, S, \Sigma_i h_i) \cdot CT(T, S, \Sigma_i h_i) \cdot |h_j|](t, lat, lon) \quad \text{Eq. 8}$$

Where

- h_j is the j-th value of the thickness layer so that $\Sigma_i h_i$ is the depth of integration (in m),
- ρ_{ref} is the reference value of the density computed at fixed Salinity (35psu) and Temperature (0°C),
- $\rho(T, S, \Sigma_i h_i)$ is the density calculated based on salinity and temperature variations,
- $\rho(T, S_{clim}, \Sigma_i h_i)$ is the density with salinity fixed at the climatology,
- $CT(T, S, \Sigma_i h_i)$ is the conservative temperature (in °C) and,
- $C_p(T, S, \Sigma_i h_i)$ is the heat capacity of sea water (in $J \cdot kg^{-1} \cdot ^\circ C^{-1}$)

We can note that, *TSSL* change and *OHC* change are locally filtered with a 3 years cut-off frequency prior to the computation of the IEEH. As it is described in Marti et al. (2022) this is done in order to remove high-frequency content related to the intrinsic ocean variability (Palmer and McNeall, 2014). In this way, the IEEH coefficient gives the Ocean Heat Content for the whole water column for a variation of thermosteric around a physical reference.

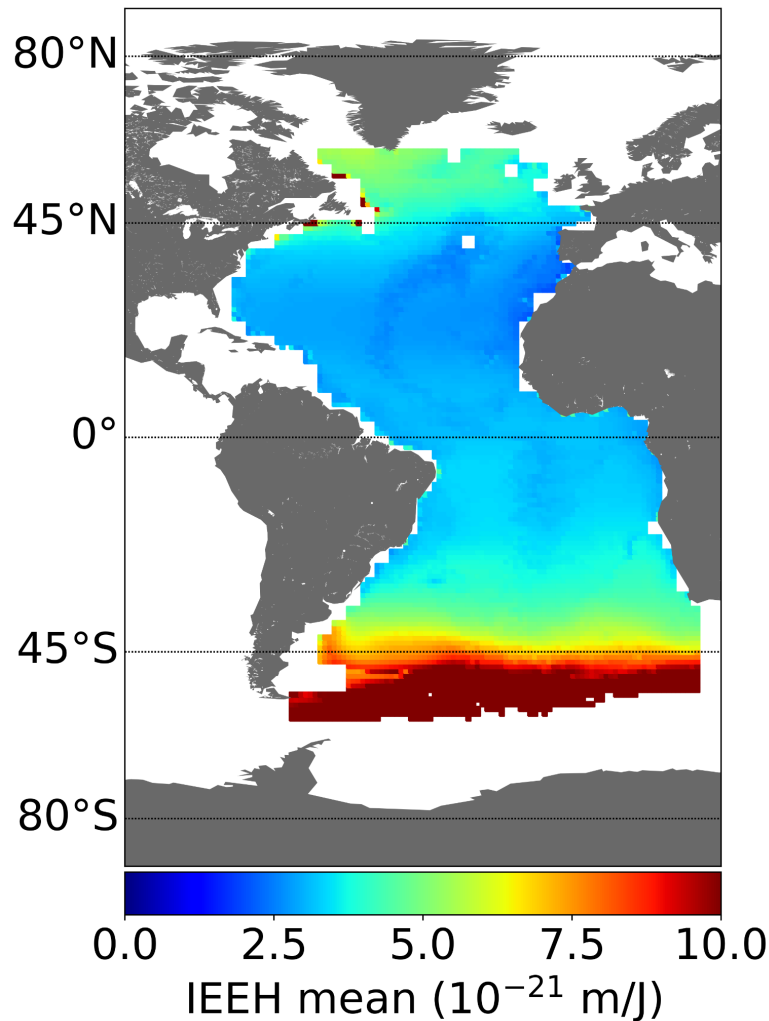


Figure 4: Time-mean of the Integrated Expansion Efficiency of Heat (IEEH) coefficients (10^{-21} m/J) (1×1 degree).

Finally, the main characteristics of IEEH grids are:

- spatial resolution: $1^\circ \times 1^\circ$
- temporal resolution: monthly
- depth integration: IFREMER ISAS20 (0-2000m) & EN4.2.2.109 (2000m-6000m)
- temporal availability: January 2002 - December 2020
- units: m/J

3.5.3. Comments/limitations

To assess the uncertainties on the OHC change derived from data at regional level, the uncertainty of the IEEH is required. For now, it has been decided to derive it from the uncertainty of the IEEH estimated at global scale in (Marti et al., 2022). This estimation results from the dispersion between several global IEEH estimated from several Argo solutions. The

method used to derive the regional uncertainty of the IEEH is explained in more detail in section [5.4.5.3](#).

3.6. Static data: water ratio

When manipulating data at regional scales, it is necessary to know the proportion of ocean in each cell for grid's downsampling or deriving the global mean for instance.

A water ratio grid is computed from distance to coast information and provides the part of water surface in each cell of the grid between 0 and 1. Distance to coast data is provided by the NASA Goddard Space Flight Center (GSFC) Ocean Color Group and given on a 0.01° resolution grid.

3.7. Static data: grid cells area

When manipulating data at regional scales, it is necessary to know the area of each cell for grid's downsampling or deriving the global mean for instance. The surface is computed for each grid cell taking the Earth oblateness into consideration.

4. 4DAtlantic OHC processing chain

4.1. Outline

The regional approach allows us to know the spatial distribution of ocean heat content change, which is essential for understanding the role of the Atlantic Ocean in the climate system.

As the OHC change is computed from the combination of altimetry-gravimetry spatial observations and the removal of the halosteric component calculated with in-situ Argo floats, its spatial and temporal characteristics depend on these measurements. OHC change characteristics will be constrained by the limitations of gravimetry observations and in-situ data both at spatial and temporal scales. Effective temporal and spatial resolutions of GRACE(-FO) products is 1 month and 300 km and it is of 1 month and 100 km for in-situ Argo products. However it is about 10-days at about 100 km for level-4 altimetry products. Therefore the regional OHC change grids in the 4DAtlantic project have been defined at $1^\circ \times 1^\circ$ resolution and on a monthly basis. As a reminder, the variables noted SL, OM and HSSL change are not absolute quantities but anomalies with respect to a reference (see sections [3.2.1](#), [3.3.1](#), [3.4.1](#)). In the following, we will define the reference of TSSL and OHC change.

The Figure 5 below describes the 4DAtlantic processing chain with its main algorithms for generating OHC data from input altimetry-gravimetry and in-situ data. The following subsections describe the algorithms developed in detail.

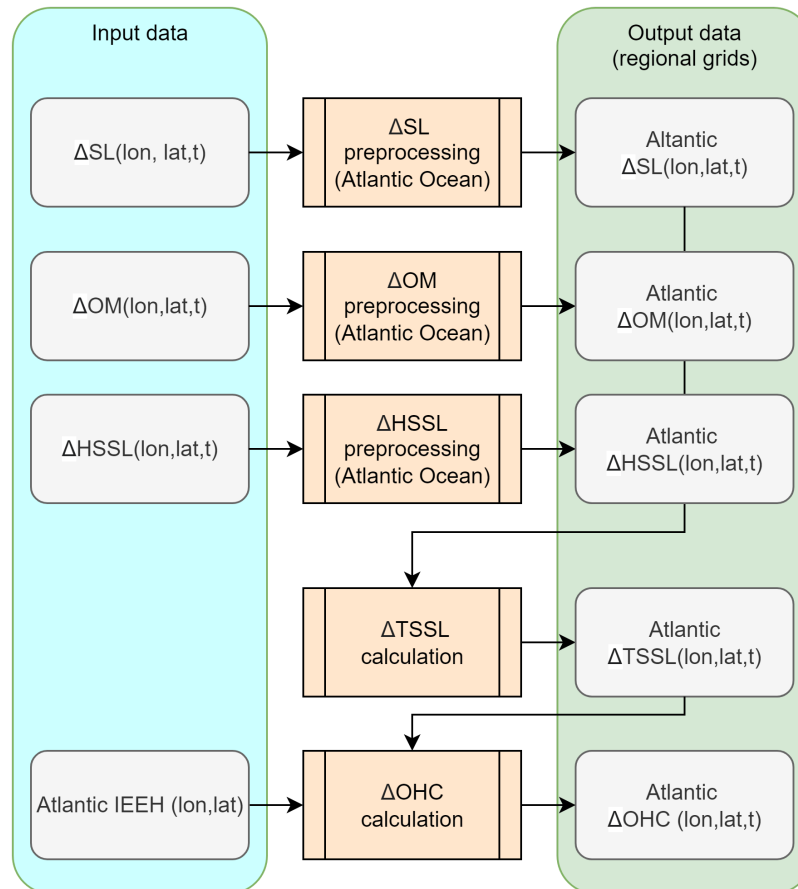


Figure 5: Overview of the 4DAtlantic processing chain. Variables are given with their dimensions (lon: longitude, lat: latitude, t: time)

4.2. Input data

The 4DAtlantic processing chain, which allows to compute the OHC change variable, is configured to use the following input data, described in section 3.

- OM change gridded data (spatial resolution: $1^{\circ} \times 1^{\circ}$ - temporal resolution: monthly)
- SL change gridded data (spatial resolution: $0.25^{\circ} \times 0.25^{\circ}$ - temporal resolution: daily)
- HSSL change gridded data (spatial resolution: $1^{\circ} \times 1^{\circ}$ - temporal resolution: monthly)
- IEEH gridded data (spatial resolution: $1^{\circ} \times 1^{\circ}$ - temporal resolution: monthly)
- land mask (spatial resolution: $1^{\circ} \times 1^{\circ}$)

4.3. Output data

The 4DAtlantic main product contains the OHC change produced by the processing chain and described in Figure 5 for each month from April 2002 to December 2020:

- OHC change grids

- Variances-covariance matrices for OHC change at every location
- OHC change quality flag (which indicates the data that are interpolated, due to gap of gravimetric data between GRACE and GRACE-FO)

The format of the 4DAtlantic product is described in detail in the 4DAtlantic Experimental Dataset Description (EDD) [Table 1, [AD1](#)].

An additional product is available upon request which contain other variables, mainly the intermediate variables (cf EDD) [Table 1, [AD1](#)].

4.4. Retrieval methodology

4.4.1. Overview

The algorithms applied in the 4DAtlantic processing chain are described in the following subsections in agreement with Figure 5:

- the preprocessing of regional SL change grids
- the preprocessing of regional OM change grids
- the preprocessing of regional HSSL change grids
- the calculation of regional TSSL change grids
- the calculation of regional OHC change grids

For each algorithm, the objectives, the main mathematical statements and the limitations and any comments about the approach are presented.

4.4.2. Preprocessing of SL change grids

4.4.2.1. Description

The objective of the preprocessing of the SL change grids is to modify the temporal and spatial resolutions of SL change grids used as input data. Indeed, altimetry data used in the 4DAtlantic processing chain is provided by C3S and are given on a daily basis at 0.25x0.25 degrees resolution. Altimetry data need to be downsampled to 1x1 degrees resolution and at the monthly time step to be compared to OM change and HSSL change grids.

Moreover, the sea level regional grids from C3S are not corrected from the glacial isostatic adjustment (GIA), the elastic effect of the contemporary land ice melting (GRD) and Jason-3 drift. To estimate OHC change, specific corrections must be applied.

4.4.2.2. Mathematical statement

Temporal interpolation

In order to calculate the SL change grids on a monthly basis (i.e. to switch from a daily to a monthly temporal resolution), a basic average of the N grids of the month is performed. Cells with default values are not taken into account. The monthly averages are kept for each cell regardless of the number of valid values over the month.

Spatial filtering

The monthly grids are first spatially filtered with a lanczos filter along the longitude and latitude coordinates. The cut-off length is chosen at 150kms and allows to filter out high frequency spatial scales in the sea level which are not present in the gravimetry and halosteric datasets.

Spatial interpolation

The monthly grids are then computed at a higher spatial resolution: 1x1 degrees instead of 0.25x0.25 degrees. The method applied consists in applying an average of the 4 cells located at the center of a box composed of 16 cells after the application of the Lanczos filter on the grids. This average will be the new value of the full 16 cells box which is 1° sided.

Corrections applied

Several corrections are applied to the sea level change grids (see section [3.3.3.](#)). The GIA unstructured ensemble mean grid is first sampled on a regular 1 degree resolution grid using linear interpolation. Regional sea level change grids are finally corrected from the GIA correction, the GRD correction and the Jason-3 drift :

$$\Delta SL(x, y, t) = GIA(x, y) - GRD(x, y) - C_{J3}(t) \quad \text{Eq. 9}$$

4.4.2.3. Comments/limitations

With regards to the GIA correction, it is still an area of active research. However the impact at regional scales is mainly significant at high latitudes (e.g. discrepancies can reach 0.5-1 mm/yr) where, for the moment, limited information is provided in the 4DAtlantic product due the application of a restrictive geographical mask based on Argo data (see below for more details).

With regards to the Jason-3 drift correction, it was derived to correct the global mean SL. Here an approximation is made by applying this correction at regional scales.

4.4.3. Preprocessing of OM change grids

4.4.3.1. Description

Gravimetry data used in the 4DAtlantic processing chain are provided at 1°x 1° resolution and monthly time step. OM change grids are already at a good spatial and temporal resolution. Hence, the objective of the preprocessing of the OM change grids is to fill the data gaps of the GRACE(-FO) in the ocean mass change grids.

4.4.3.2. Mathematical statement

Management of the data gap

The OM change grids contain several gaps due to degradation of the operational capability of GRACE and GRACE-FO and the transition time between the two missions. An implementation of

a gap filling algorithm has been made in the product chain generation. This algorithm is described as follows:

- Calculation of the climatological signal: removal of the trend and calculation of the average for each month of the year
- Removal of the climatological signal over the whole time series
- Cubic approximation of the time series to fill in the gaps
- Adding the climate signal to the whole time series (including the gap)

This gap filling algorithm has been applied at regional scales, i.e for each element of the OM change grids.

An important feature brought by the gap algorithm to the OHC change product is a quality flag which distinguishes between months for which there is data from observations and those for which there is data from interpolation of OM change. A more detailed explanation of this quality flag is given in the EDD [Table 1, [AD1](#)].

Addition of a high frequency component into the data gaps

The gap-filling algorithm underestimates the part of the signal driven by sub-annual processes. By construction, the high frequency content of the GMOM uncertainty estimates in the data gaps are also underestimated. To deal with that problem, prior to the calculation of the variance-covariance matrix (section [5.4.2.](#)), some modifications were directly made onto the signals of the ensemble of ocean mass solutions. The high frequency related signal component was added to the ensemble signals as follows:

- Application of a 1-year filter onto OM data with prior removal of the annual and semi-annual components of the signal
- Calculation of the standard deviation of the difference between the initial and filtered OM signal
- Stochastic addition with a normal (Gaussian) distribution of this residual standard deviation at the locations where the OM is suffering from a lack of data

Note that this method is applied to all the data gaps on the full time period.

4.4.3.3. Comments/limitations

The spatial interpolation method applied is simple. More sophisticated algorithms could be applied to account for data gaps in the time series. Such methods based on the filter approach (e.g. Gaussian filter for spatial interpolation) are planned in future versions of the OHC change products. The impact on these improved algorithms is unknown at this time.

4.4.4. Preprocessing of HSSL change grids

4.4.4.1. Description

Halosteric sea level change data used in the 4DAtlantic processing chain are provided at 1°x 1° resolution and monthly time step. HSSL change grids are already at a good spatial and temporal resolution. No modification has been brought to the grids during their preprocessing.

4.4.5. Calculation of regional TSSL change grids

4.4.5.1. Description

The objective is to calculate the regional TSSL change grids from SL, OM and HSSL change grids. The relationship between sea level change (ΔSL), ocean mass change (ΔOM) and steric sea level change (ΔSSL) is expressed by the sea level budget equation:

$$\Delta SL = \Delta SSL + \Delta OM \quad \text{Eq. 10}$$

It is known that the steric sea level change can be divided into the sum of thermosteric sea level change ($\Delta TSSL$) and halosteric sea level change ($\Delta HSSL$):

$$\Delta SSL = \Delta TSSL + \Delta HSSL \quad \text{Eq. 11}$$

When corrected for changes in ocean mass and halosteric component, sea level change provides an estimate of the thermal expansion of the ocean ($\Delta TSSL$).

4.4.5.2. Mathematical statement

The TSSL change grids are obtained from removing the OM and HSSL change grids to SL change grids at each time step. As SL, OM and HSSL change grids have been preprocessed at same spatial and temporal resolution, the differences between grids is straightforward:

$$\Delta TSSL(lon, lat, t) = \Delta SL(lon, lat, t) - \Delta OM(lon, lat, t) - \Delta HSSL(lon, lat, t) \quad \text{Eq. 12}$$

For each cell containing a default value in the SL, OM or HSSL change grids, a default value is assigned in the TSSL change grids.

4.4.5.3. Comments/limitations

Other alternative methodologies are used to derive the thermosteric sea level grids. They rely on in situ data instead of spatial data, mainly from temperature and salinity profiles provided by the Argo network. The advantages and inconvenients of such an approach is presented in Meyssignac et al. (2019).

Thermosteric sea level is obtained by subtraction of signals. Some limitations related to this operation can be identified. The GIA datasets used to correct the gravimetry signals and the sea level from altimetry are not consistent (three different GIA corrections for the post-processing of gravimetry solutions and one solution for altimetry, see sections [3.2.](#) and [4.4.2.1.](#)). To date, the impact of such incoherency in the processing of data is expected to be low. However, a possible homogenisation of the pre-processing of altimetry and gravimetry

datasets should solve this issue. Finally, the dynamical atmospheric correction based on MOG2D model (Carrère and Lyard, 2003) has been removed in altimetry processing whereas only the inverse barometer correction has been applied in gravimetry processing (Blazquez et al., 2018). The impact of this discrepancy must be studied and corrected if needed.

4.4.6. Calculation of regional OHC change grids

4.4.6.1. Description

The objective is to calculate the regional OHC change grids from TSSL grids at the same spatial and temporal resolution. Once the IEEH variable is determined at regional scale, TSSL change is translated to OHC change thanks to the IEEH at every timestep.

4.4.6.2. Mathematical statement

In order to get the ocean heat content change (in Joules), we divide all grids of steric sea level changes (m) by the regional IEEH grid ($\text{m}\cdot\text{J}^{-1}$). According to the Equation 1 given in section 2.2., the OHC change is expressed per unit of area ($\text{J}\cdot\text{m}^{-2}$), when dividing by the reference surface:

$$\Delta OHC(lon, lat, t) = \frac{\Delta TSSL(lon, lat, t) + TSSL_{ref}(lon, lat)}{surf_{cell}(lon, lat) * IEEH(lon, lat, t)} - \frac{TSSL_{ref}(lon, lat)}{surf_{cell}(lon, lat) * IEEH(lon, lat, t_{ref})} \quad \text{Eq. 13}$$

where $surf_{ref}$ is defined as the surface of each cell.

It results in monthly OHC change given on a $1^\circ \times 1^\circ$ resolution grid. For each cell containing a default value in the TSSL or IEEH grids, a default value is assigned in the OHC grids.

4.4.6.3. Comments/limitations

The OHC change calculation requires a reference value for the TSSL. In order for this reference value to be consistent with the IEEH value in Equation 13, it is set equal to the TSSL value used to compute the IEEH and obtained from in-situ measurements. The reference date is fixed $t_{ref} = 01/2005$, thus $TSSL_{ref}(lat, lon) = TSSL_{in-situ}(t = 01/2005, lat, lon)$. A sensitivity study has been led on the choice of the date or period of reference and the associated $TSSL_{ref}$ value. The results have shown no significant impact on the OHC change calculation and the time derivative of the OHC change.

The grid containing the regional IEEH coefficients was calculated from the temperature and salinity profiles derived from the Argo network (Marti et al., 2022). Consequently, this grid is not defined in coastal areas (with bathymetry less than 700 m) and in high latitudes. This is currently a limitation as it prevents from calculating the regional OHC change over the whole sea surface. In the future, one solution could be found to extrapolate this grid in a realistic way and estimate the variations of the OHC change over almost all oceans.

5. Uncertainties calculation and propagation

5.1. Overview

In parallel to the product processing described in the previous section, the uncertainties are calculated and provided at each location for : SL, OM, HSSL, TSSL and OHC change. The proposed approach consists in providing a variance-covariance matrix (Σ) of the errors for at every location in the Atlantic Ocean. Once the variance-covariance matrices are known, the trend uncertainties can be derived for any location and time spans of the time series. It is also possible to make it for any other indicators such as the mean, the acceleration or the magnitude of the annual signals at every location for instance. The method for deriving regional uncertainties is based on Prandi et al. (2021) for the sea level trends and accelerations. This method does not take into account spatial correlations. As a matter of fact we will work with temporal correlations only.

The Figure 6 below describes main steps to propagate the uncertainties from the SL and OM change grids until the OHC change grids. As we just consider time correlated errors, variance-covariance matrices are computed and propagated for every latitude and longitude couple.

The following subsections described the algorithms developed in detail.

For now, the variance-covariance matrices are computed at annual resolution.

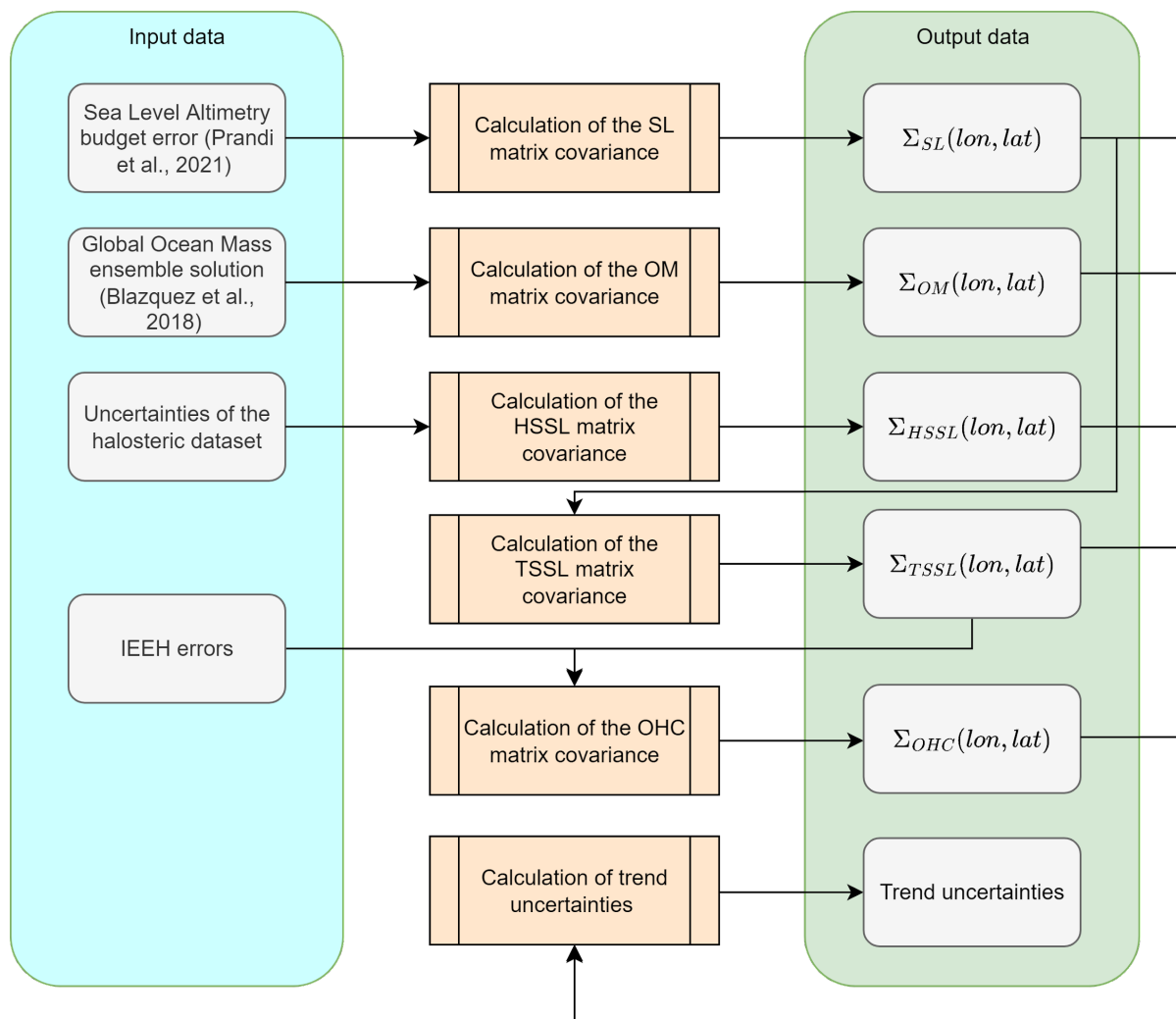


Figure 6: Uncertainty calculation and propagation chain

5.2. Input Data

The input data used are:

- the sea level altimetry regional error budget given by (Prandi et al., 2021) and its associated variance-covariance matrix (displayed on table below),
- the ensemble of ocean mass solutions provided by Blazquez et al. (2018) available in NetCDF format file on the LEGOS ftp site [Table 2, RD4].
- land mask (spatial resolution: 1° x 1°)

- the uncertainty of the thermal expansion of heat coefficient provided by Marti et al. (2022): $5.5 \cdot 10^{-4} m. YJ^{-1}$

Source of errors	Error category	Uncertainty level (at 1 σ)
High frequency errors: altimeter noise, geophysical corrections, orbits ...	Correlated errors ($\lambda = 1$ year)	$\sigma =$ location dependent
Low frequency errors: wet tropospheric correction	Correlated errors ($\lambda = 10$ years)	$\sigma =$ location dependent
Drift errors from the orbit determination	Drift error	$\delta = 0.33$ mm/yr
Drift errors from the GIA correction	Drift error	$\delta =$ location dependent
inter-mission TP-a/TP-b and TP-b/J1 biases	Jump	$\Delta = 10$ mm
inter-mission J1/J2 and J2/J3 biases	Jump	$\Delta = 6$ mm

Table 4: Altimetry regional error budget given at 1-sigma

5.3. Output Data

Errors are characterised with the following variance-covariance matrices:

- $\Sigma_{SL}, \Sigma_{OM}, \Sigma_{HSSL}$ and Σ_{TSSL} for the SL, OM, HSSL and TSSL
- Σ_{OHC} for the OHC

5.4. Retrieval methodology

5.4.1. Calculation of the SL covariance matrix

5.4.1.1. Description

For now, the error variance covariance matrix of SL (Σ_{SL}) is the one provided in (Prandi et al., 2021). It is deduced from the regional sea level error budget described in Table 4 and computed at annual resolution. Thus, for each $(nlat, nlon)$ couple, a square matrix of variance-covariance is calculated with the dimensions $(ntime, ntime)$. The final object which

contains all the variance-covariance matrices have the following dimensions:
 $\Sigma_{SL}(nlat, nlon, ntime, ntime)$

5.4.1.2. Mathematical statement

As it was assumed that all error sources shown in Table 4 are independent one to each other. The matrix is the sum of the individual variance-covariance matrices of each error source in the sea level error budget:

$$\Sigma_{SL} = \sum_{i=1}^n \Sigma_{Error_i} \quad \text{Eq. 14}$$

5.4.1.3. Comments/Limitations

This matrix is based on the current knowledge of altimetry measurement errors. As the altimetry record increases in length with new altimeter missions, the knowledge of the altimetry measurement also increases and the description of the errors improves. Consequently, the error variance-covariance matrix is expected to change and improve in the future – hopefully with a reduction of measurement uncertainty in new products.

It is also important to note that the error budget approach applied here to derive the variance-covariance matrix is conservative. In other words, sea level altimetry errors may be overestimated with respect to reality.

More information is given in (Prandi et al., 2021).

5.4.2. Calculation of the OM covariance matrix

5.4.2.1. Description

The objective is to calculate the error variance-covariance matrix of the OM grids (Σ_{OM}) for the time period of the study (also at annual resolution by computing the annual mean of the ensemble). Σ_{OM} is derived from an OM ensemble deduced from the ensemble of ocean mass solutions provided by Blazquez et al. (2018), containing 288 GRACE(-FO) grids datasets.

5.4.2.2. Mathematical statement

The OM data from GRACE(-FO) are available worldwide. Only ocean data is kept by applying the land mask. For each latitude and longitude of the OM ensemble, the regional variance-covariance matrix is computed by using all the solutions of the ensemble for this given location.

The resulting OM ensemble solutions contains n temporal vectors noted hereafter X_i for i=1 from 1 to n. The variance-covariance matrix (Σ_{OM}) is the matrix whose entry is the covariance:

$$\Sigma_{OM}(i, j) = cov(X_i, X_j) = E[(X_i - E[X_i])(X_j - E[X_j])]$$

where E is the mean operator.

5.4.2.3. Comments/Limitations

The ensemble provided by Blazquez et al. (2018) contains 288 solutions which is a important number of solutions to calculate Σ_{OM} . However the mathematical formulation above assumes a normal distribution of the different OM solutions. In practice, it is not fully the case. Thorough investigations must be performed to analyse the impact of this approximation.

In contrast to altimetric sea level errors, the ensemble error approach applied here to derive a variance-covariance matrix could be considered as an optimistic view of the OM error description. This means that OM regional uncertainties could be underestimated.

5.4.3. Calculation of the HSSL covariance matrix

The objective is to calculate the regional variance-covariance of the HSSL, for now the only uncertainties that we have are the ones on temperature and salinity profiles from EN4 and ISAS20 data. The propagation of these uncertainties to the HSSL is not easy to implement and need further investigations. Thus, it has been decided to neglect the HSSL uncertainties and set the variance-covariance matrix of HSSL (Σ_{TSSL}) to 0. This means that OHC regional uncertainties could be underestimated.

5.4.4. Calculation of the TSSL covariance matrix

5.4.4.1. Description

The objective is to compute the variance-covariance matrix of the TSSL errors (Σ_{TSSL}). As TSSL is obtained by calculating the differences between SL, OM and HSSL, Σ_{TSSL} is obtained by summing the variance-covariance matrices of the errors of SL, OM and HSSL. Indeed, since the errors of the three data sets are considered independent (see limitations section below), the errors are additive.

5.4.4.2. Mathematical statement

Σ_{TSSL} is the sum of Σ_{SL} , Σ_{HSSL} and Σ_{OM} .

5.4.4.3. Comments/Limitations

The proposed method for calculating the TSSL error variance-covariance matrix from the sum of the SL, OM and HSSL error variance-covariance matrix are based on two main assumptions :

- SL, OM, and HSSL are assumed independent: this assumption is based on the fact that sensor are fully independent but in practice similar geophysical corrections are applied in their on-ground processing (e.g. GIA and ocean tide to calculate SL and OM change) which can generate correlated errors not quantified to date. However we expect such error correlations to be negligible.

- Potential errors due to the collocation between the datasets (SL, OM, HSSL) have not been taken into account and the different sensors may not be able to observe the same signals due to their spatial and temporal coverage. Such studies must be performed in the future to evaluate this source of uncertainty.

5.4.5. Calculation of the OHC covariance matrix

5.4.5.1. Description

The objective is to calculate the variance-covariance matrix of the OHC change errors (Σ_{OHC}). The errors from TSSL time series are propagated to the OHC change time series taking into account the relationship between the OHC and TSSL change via the regional integrated expansion efficiency of heat coefficient (ϵ or IEEH) and its uncertainty (e_ϵ). Σ_{OHC} is inferred from Σ_{TSSL} from the following relationship (see details in next subsection).

$$\Delta OHC(t, lat, lon) = \frac{\Delta TSSL(t, lat, lon) \pm e_{TSSL}(t)}{\epsilon(t, lat, lon) \pm e_\epsilon} \quad \text{Eq. 15}$$

5.4.5.2. Mathematical statement

In case of two uncorrelated scalar variables a and b, with a respective uncertainty e_a and e_b , the error propagation division follows the ensuing relationship (Taylor, 1997, equation 3.8):

$$\left(e_{\frac{a}{b}}\right)^2 = \left(\frac{1}{b}\right)^2 * \left[e_a^2 + \left(e_b * \frac{a}{b}\right)^2\right] \quad \text{Eq. 16}$$

In our case:

- a= TSSL(t, lat,lon) and e_a is $e_{SSL}(t, lat, lon)$
- b= IEEH (noted ϵ) and e_b is given by e_ϵ
- $\frac{a}{b} = \frac{\Delta TSSL(t, lat, lon)}{IEEH(t, lat, lon)} = \Delta OHC(t, lat, lon)$

Thus with these notations, the first equation becomes:

$$(e_{\Delta OHC(t, lat, lon)})^2 = \frac{1}{\epsilon(t, lat, lon)^2} * (e_{\Delta TSSL(t, lat, lon)})^2 + \left(\frac{e_{\epsilon}}{\epsilon(t, lat, lon)}\right)^2 * (\Delta OHC(t, lat, lon))^2 \quad \text{Eq. 17}$$

which can be written in matricial notation with the variance-covariance matrices Σ_{OHC} and Σ_{TSSL} (containing the uncertainties e_{OHC}^2 and e_{TSSL}^2 respectively) as follows:

$$\Sigma_{\Delta OHC(lat, lon)} = \frac{1}{\epsilon(lat, lon)^2} \Sigma_{\Delta TSSL(lat, lon)} + \left(\frac{e_{\epsilon}}{\epsilon(lat, lon)}\right)^2 \Delta OHC(lat, lon) * \Delta OHC(lat, lon)^T \quad \text{Eq. 18}$$

5.4.5.3. Uncertainties of the regional IEEH

As the IEEH is not an intensive parameter (i.e. it can not be averaged from regional scale to global scale), it is not suitable to take the uncertainty associated with the global IEEH (Marti et al., 2022) at regional scales. The uncertainties of the regional IEEH are derived from the one of the global IEEH with the following formula:

$$e_{\epsilon}(lat, lon) = \frac{\epsilon(lat, lon) * e_{\epsilon_{global}}}{\epsilon_{global}} \quad \text{Eq. 19}$$

In the above equation, $e_{\epsilon}(lat, lon)$ is the uncertainty at a given latitude and longitude. It is calculated thanks to $\epsilon(lat, lon)$ the values of the IEEH from Figure 4, $e_{\epsilon_{global}} = 5.5 \cdot 10^{-4} m.YJ^{-1}$ the uncertainty of the IEEH at global scale (Marti et al., 2022) and $\epsilon_{global} = 1.68 \cdot 10^{-25} mJ^{-1}$ the value of the IEEH calculated at global scale for the in-situ product used in the framework of this project.

5.4.5.4. Comments/Limitations

In this formalism, it has been decided to use the uncertainty of the global IEEH rather than the uncertainty of local IEEH.

The mathematical formalism proposed for the propagation of errors from the TSSL change to the OHC change shows that the errors of the OHC change depend both on the uncertainty of the value of the IEEH coefficient and on the value of the coefficient itself. When analysing the impact of changing this coefficient and its uncertainty (from Levitus et al., 2012/Kuhlbrodt and Gregory, 2012 to Marti et al., 2022), we found that this significantly reduced OHC change uncertainties.

5.4.6. Calculation of trend uncertainties

5.4.6.1. Description

The objective is to calculate the trend uncertainty, adjusting a polynomial of degree 1 by an ordinary least square (OLS) method taking into account the error variance-covariance matrix for the calculation of the uncertainty.

5.4.6.2. Mathematical statement

The ordinary least square (OLS) regression method is used in this study. The estimator of β with the OLS approach is noted:

$$\hat{\beta} \sim (X^t X)^{-1} X^t y \quad \text{Eq. 20}$$

where y is the vector containing the observations (e.g. SL change, OHC change, ... at each location) and X the vector containing the dates of the observations.

The uncertainty in the trend estimates takes into account the correlated errors of the observations (y). So, the error is integrated into the trend uncertainty estimation. Taking into account the variance-covariance matrix (Σ), the estimator of β becomes:

$$\hat{\beta} = N(\beta, (X^t X)^{-1} (X^t \Sigma X) (X^t X)^{-1}) \quad \text{Eq. 21}$$

5.4.6.3. Comments/Limitations

As we just consider time correlated errors and not the spatial errors, the inversion of the matrix is done on the $nlat * nlon$ square matrices of dimension $(ntime, ntime)$.

The proposed approach is also applicable for any other adjusted variables. For instance, the acceleration of the time series can be calculated from the adjustment of a polynomial of degree 2 ($a_0 + a_1 X + a_2 X^2$) where the acceleration (a) is given by $a = 2a_2$. The uncertainty acceleration is calculated applying the same mathematical formalism described previously for the trend.